Catalysis Today 139 (2008) 2–7

Contents lists available at ScienceDirect

Catalysis Today

journal homepage: www.elsevier.com/locate/cattod

Enhanced activity of Ca-doped Cu/ZrO_2 for nitrogen oxides reduction with propylene in the presence of excess oxygen

Dong Yang [a,b], Junhua Li [a,*], Mingfen Wen [b], Chongli Song [b]

[a] Department of Environment Science and Engineering, Tsinghua University, Beijing 100084, China
[b] Institute of Nuclear and New Energy Technology, Tsinghua University, Beijing 102201, China

ARTICLE INFO

Article history:
Available online 21 September 2008

Keywords:
Nitrogen oxides
SCR
Copper
Zirconia
Calcium
Alkaline-earth metals

ABSTRACT

In this work, the effect of adding alkaline-earth metals (Mg, Ca, Sr, and Ba) to the ZrO_2 support on the activity of Cu/ZrO_2 catalyst for selective catalytic reduction (SCR) of NO_x with C_3H_6 was investigated. The catalytic activity of Cu/ZrO_2 was greatly enhanced by the addition of 5% all of the four alkaline-earth metals to the ZrO_2 support. The highest promotional effect was observed over the Ca-modified Cu/ZrO_2 catalyst. BET, H_2-TPR and DRIFTS results revealed that the $Cu/CaZrO_2$ catalyst had a better metal dispersion and metal–support interaction than Cu/ZrO_2 catalyst. This feature inhibited the direct oxidation of C_3H_6 and improved the C_3H_6 selectivity for the reduction of NO. On the other hand, NO_x-TPD and DRIFTS results showed that $Cu/CaZrO_2$ catalyst could adsorb much more nitrate species than Cu/ZrO_2 catalyst under both static room temperature adsorption and the real reaction conditions, while nitrate species was an important intermediate in the C_3H_6-SCR.

1. Introduction

Selective catalytic reduction (SCR) of nitrogen oxides with hydrocarbons is an efficient way to remove NO in the presence of excess oxygen. Efficiency of copper-based zeolite or metal oxide catalysts for the reaction has been substantially investigated in the past. A large amount of studies have been devoted to the characterization of Cu-ZSM5 [1–3], Cu/Al_2O_3 [4–7], Cu/ZrO_2 [8–10], and Cu/SiO_2 [11,12] catalysts.

Many of the investigations on copper-based catalysts have studied dispersion and the coordination state of copper. There is much evidence that isolated copper ions are the active sites for the SCR with hydrocarbons, and small CuO crystallites can reduce the activity of catalyst. In Cu-ZSM-5, NO conversion increases with the extent of exchanged Cu-ZSM-5 up to 100%. Compared with the 100% exchanged Cu-ZSM-5, zeolite with high Cu content containing segregated CuO, have lower activity [2]. For the Cu/ZrO_2 catalyst, the turnover frequency (NO molecules converted per second per Cu atom) was almost independent on the Cu content, up to about 2.5 atoms nm^{-2}, that is, copper can be uniformly dispersed on the ZrO_2 surface below the limit content [9]. The limits of uniform Cu dispersion of Cu/Al_2O_3 and Cu/SiO_2 catalysts are 3.2 and 1.7 atoms nm^{-2} [13,14], respectively.

For the purpose of improving the activity of copper-based catalyst for HC-SCR, many researchers chose the route of adding additives to promote the dispersion of copper species. By investigating the effect of Ag and Cr on the activity of Cu/CeO_2 catalyst, Amin et al. [15,16] found that co-loading of Ag, Cu or Cr, Cu could improve the dispersion of copper species over the surface of CeO_2. As a result, the NO reduction activity of Cu/CeO_2 was improved from 40 to 80%. On the other hand, increasing the acidity of support can also lead to a improved dispersion of copper species. Since the strong interaction between acid sites over support and copper can prevent the copper aggregation [17]. For example, Bennici et al. [18] successfully improved NO conversion activity of the Cu/SiO_2 catalyst through an increase in the acidity of the support by modifying Cu/SiO_2 with Al and Zr. Another example is the SO_4^{2-} modified Cu/ZrO_2 catalyst [19]. Introducing SO_4^{2-} into Cu/ZrO_2 catalyst can substantially improve the SCR activity, because the acidic property of Cu/ZrO_2 was highly improved by SO_4^{2-}.

In this paper, alkaline-earth elements (Mg, Ca, Ba, and Sr) were selected as additives to improve the activity of Cu/ZrO_2 catalyst for C_3H_6-SCR. It was found all the four additives, especially Ca, showed significant improvement on the activity of Cu/ZrO_2 catalyst. The attention was mainly focused on the effect of Ca, especially on its promotional effect on the copper dispersion and NO_x adsorption of Cu/ZrO_2 catalyst.

* Corresponding author. Tel.: +86 10 62782030; fax: +86 10 62785687.
E-mail address: lijunhua@tsinghua.edu.cn (J. Li).

0920-5861/$ – see front matter © 2008 Elsevier B.V. All rights reserved.
doi:10.1016/j.cattod.2008.08.002

2. Experimental

2.1. Catalyst preparation

The alkaline-earth elements doped to the zirconia supports were prepared by the co-precipitation method. The mixed solution of $Zr(NO_3)_4$ and corresponding alkaline-earth element nitrates were added drop by drop to ammonia solution at room temperature with vigorous stirring. The precipitate was stirred for further 2 h, filtered, and then washed with deionized water until the pH reached 7.0. The resultant material was dried at 120 °C for 14 h, and then calcined at 550 °C for 5 h in air. The individual ZrO_2 support was prepared in a similar way.

The copper supported catalysts were prepared through wet impregnation at ambient temperature with aqueous $Cu(NO_3)_2$ solution as the copper precursor. The catalysts were then dried at 120 °C for 15 h and calcined at 550 °C for 5 h. The resulting catalysts are hereafter referred to as Cu*aMb*Zr; *a*, *M*, *b*, refer to the weight content of Cu, the alkaline-earth element, and the atom content of the alkaline-earth element in the supports, respectively. For comparison, a sulfated Cu/ZrO_2 catalyst was prepared by impregnating ZrO_2 with $CuSO_4$. This catalyst is referred to as SO_4CuZr. Prior to the catalytic performance test, all catalysts were ground to the 60–80-mesh size.

2.2. Catalytic performance test

The NO reduction activity measurements were carried out in a fixed-bed quartz reactor with an inner diameter of 4 mm using 0.2 g catalyst. The feed gas mixture contained 2000 ppm NO, 2000 ppm C_3H_6, 2% O_2 and helium as the balance gas. The total flow rate of the feed gas was 120 cm^3 min^{-1}. The composition of the product gas was analyzed using gas chromatography (equipped with porapak Q and molecular-sieve 5A columns). A molecular-sieve 5A column was used for the analysis of N_2 and CO, and a porapak Q column for analysis of N_2O, CO_2 and C_3H_6. The activity data were collected when the catalytic reaction reached an steady-state condition at each temperature. The percent selectivities of S_{scr} (NO_x reduction rather than C_3H_6 combustion) were calculated as: $S_{scr} = 100 \times (1/2)NO_x$ converted/C_3H_6 converted.

2.3. Catalyst characterization

X-ray diffraction patterns (XRD) were obtained using a Rigaku D/max-RB diffractometer. Analysis were performed with Cu target (40 kV and 100 mA); a typical scan speed was 6° min^{-1} with a step of 0.002° in the range from 20° to 70°. BET surface area, pore size, and pore volume were measured by N_2 adsorption–desorption method using a NOVA 3200e analyzer.

H_2-TPR was performed in a quartz microreactor, and 50 mg sample was used in each measurement. The samples were first pre-treated under an air flow at 500 °C for 1 h, followed by purging with N_2 at the same temperature for 1 h and cooling to room temperature. The flow of 5% H_2 in N_2 (30 mL min^{-1}) was then switched into the system, and the sample was heated to 400 °C at room temperature at a rate of 10 °C min^{-1}. The amount of H_2 uptake during the reduction was measured by a thermal conductivity detector (TCD), which was calibrated by the quantitative reduction of CuO to the metallic copper.

Temperature programmed desorption (TPD) experiments of NO_x were carried out using 100 mg of a sample in a quartz reactor with an internal diameter of 8 mm. The sample was pre-treated in a flow of 10% O_2/N_2 (100 mL min^{-1}) at 600 °C for 1 h and then cooled to room temperature under the same gas flow. Adsorption of NO_x was performed by passing a flow of 1000 ppm NO and 10% O_2 diluted in N_2 (100 mL min^{-1}) through the sample bed at room temperature for 1 h. After the adsorption gas NO_x was purged to an undetectable level in the effluent, TPD measurements were carried out up to 600 °C at a heating rate of 10 °C min^{-1} in the flowing N_2. The gas flow rate was fixed at 100 mL min^{-1}.

In situ DRIFTS spectra were recorded on a NEXUS 870-FTIR equipped with a smart collector and an MCT/A detector cooled by liquid N_2. The samples for studies were finely ground and placed in a ceramic crucible. Prior to each experiment, the catalysts were heated in a flow of 10% $O_2 + N_2$ for 60 min at 600 °C, and then cooled to the desired temperature. A spectrum of the catalyst in the flow of N_2 served as the background and was recorded. All of the spectra were measured under actual reaction conditions with a resolution of 4 cm^{-1} and an accumulation of 100 scans.

3. Results and discussion

3.1. Activity measurements

3.1.1. Effect of additives on the activity of Cu/ZrO_2

The impact of alkaline-earth metal additives on the activity of CuZr catalyst is presented in Fig. 1. It can be seen from Fig. 1a that the maximum NO_x conversion over the CuZr catalyst was only 42%, which is in agreement with the result reported by Pietrogiacomi et al. [9]. In contrast, samples with the addition of Ca, Ba, and Sr to the support of the CuZr catalyst exhibited remarkable improvement in the NO_x reduction activity, especially for the CuCaZr catalyst, over which the maximum NO_x conversions above 70% were reached at 350 °C. As shown in Fig. 1b C_3H_6 oxidation activities over the alkaline-earth metal doped catalysts were lower than that on the undoped CuZr catalyst. The results indicated that the oxidation capacity of copper species over the doped catalyst was reduced in comparison with the CuZr catalyst. As a result of this fact, the maximum NO_x conversions of these doped catalysts shifted by 25 °C to higher temperature than the CuZr catalyst. The selectivity S_{scr} of these catalysts is given in Fig. 1c. All of the alkaline-earth metal doped catalysts showed superior selectivity to that of CuZr catalyst, and the selectivity S_{scr} of CuCaZr was the highest among the four modified catalysts.

For comparative purposes, the activity of SO_4^{2-} modified CuZr was also tested, and the results are shown in Fig. 1. Maximum NO_x conversion over the SO_4CuZr catalyst was 55% at 375 °C. This performance was inferior to each of the alkaline-earth metal doped catalysts. In the further investigations, the emphasis was focused on the effect of Ca on the activity of CuZr catalyst.

3.1.2. Effect of Ca loading on the activity of $Cu/CaZrO_2$

The effect of varying the Ca content from 2 to 20% on the performance of Cu0.8CaZr catalyst is shown in Fig. 2. Compared with CuZr catalyst activity (Fig. 1), it can be seen that the maximum NO_x conversion activity was generally improved from 42 to 76% with the increase of Ca content from 0 to 5%. Further increasing the Ca content led to a decrease of the activity. However, the NO_x conversion of 48% over CuCa20Zr catalyst was still higher than the activity of CuZr catalyst. On the other hand, C_3H_6 conversion activities of CuCaZr catalysts were generally reduced with the increase of Ca content. In Fig. 2c CuCaZr catalysts showed the highest selectivity S_{scr} with the Ca content of 5%. Therefore, the optimal additive Ca loading for CuZr catalyst was 5%.

3.1.3. Effect of Cu loading on the activity of $Cu/Ca–ZrO_2$

Fig. 3 shows the extended investigation of the Cu content impact on CuCa5Zr catalysts. It can be seen that with the increasing of Cu content, the maximum NO_x conversion over the CuCaZr increased initially, then decreased. Moreover, maximum NO_x

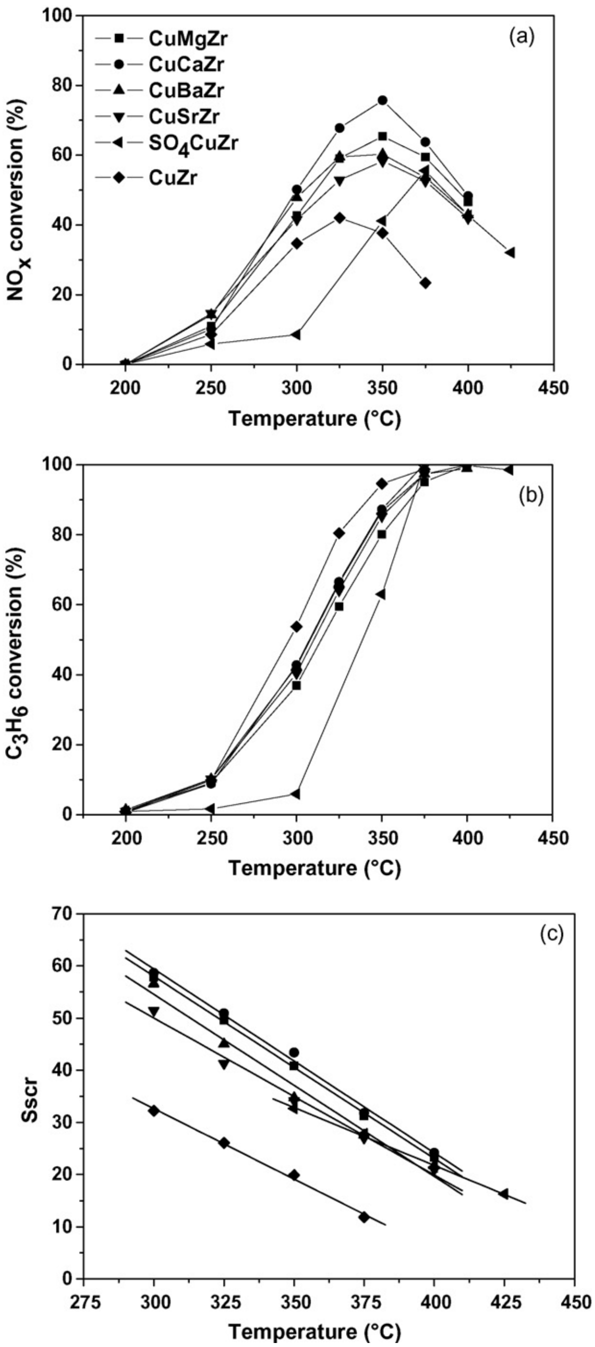

Fig. 1. Effect of adding alkaline-earth metal and SO_4^{2-} to Cu/ZrO_2 on (a) NO_x conversion, (b) C_3H_6 conversion, and (c) the selectivity S_{scr}. The loading of Cu over all of these catalysts was 0.8 wt%, and the contents of alkaline-earth metals in the supports were 5 at.%. Catalyst weight 0.2 g, feed: 2000 ppm NO, 2000 ppm C_3H_6, 2% O_2, He balance and 120 mL min^{-1} total flow.

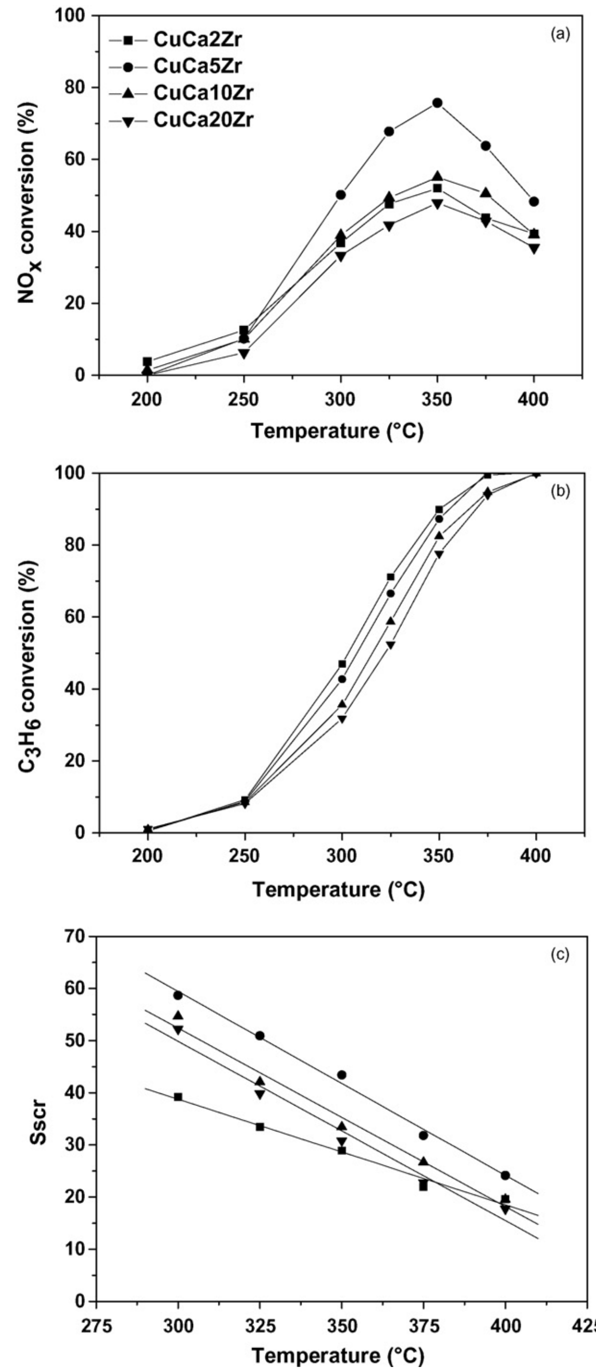

Fig. 2. Effect of adding various Ca loading weights to CuZr on (a) NO_x conversion, (b) C_3H_6 conversion, and (c) the selectivity S_{scr}. The loading of Cu over all of these catalysts was 0.8 wt%. Catalyst weight 0.2 g, feed: 2000 ppm NO, 2000 ppm C_3H_6, 2% O_2, He balance and 120 mL min^{-1} total flow.

conversion was obtained at lower temperature. Fig. 3b shows that the conversion of C_3H_6 increased with the Cu content, indicating that the accumulation of Cu species accelerated the side reaction of combustion, which resulted in the decrease in the selectivity of CuCaZr catalysts at high Cu loading (Fig. 3c).

3.2. Catalyst characterization

3.2.1. Pore structure

The BET results of CuZr and alkaline-earth metal modified CuZr catalysts are summarized in Table 1. All of CuMgZr, CuCaZr, CuBaZr, and CuSrZr catalysts showed much higher surface area than CuZr catalysts in the order: CuCaZr > CuSrZr > CuBaZr > CuMgZr. The increase in the surface area of support can improve the dispersion of Cu species over these catalysts, and this might be an important reason for the improvement in activity.

3.2.2. XRD

XRD patterns of all CuZr catalysts and alkaline-earth metals modified CuZr catalysts are shown in Fig. 4. For ZrO_2 supported catalysts, monoclinic ZrO_2 was the only observed phase, as shown for Cu0.8Zr in Fig. 4. For alkaline-earth metals modified ZrO_2

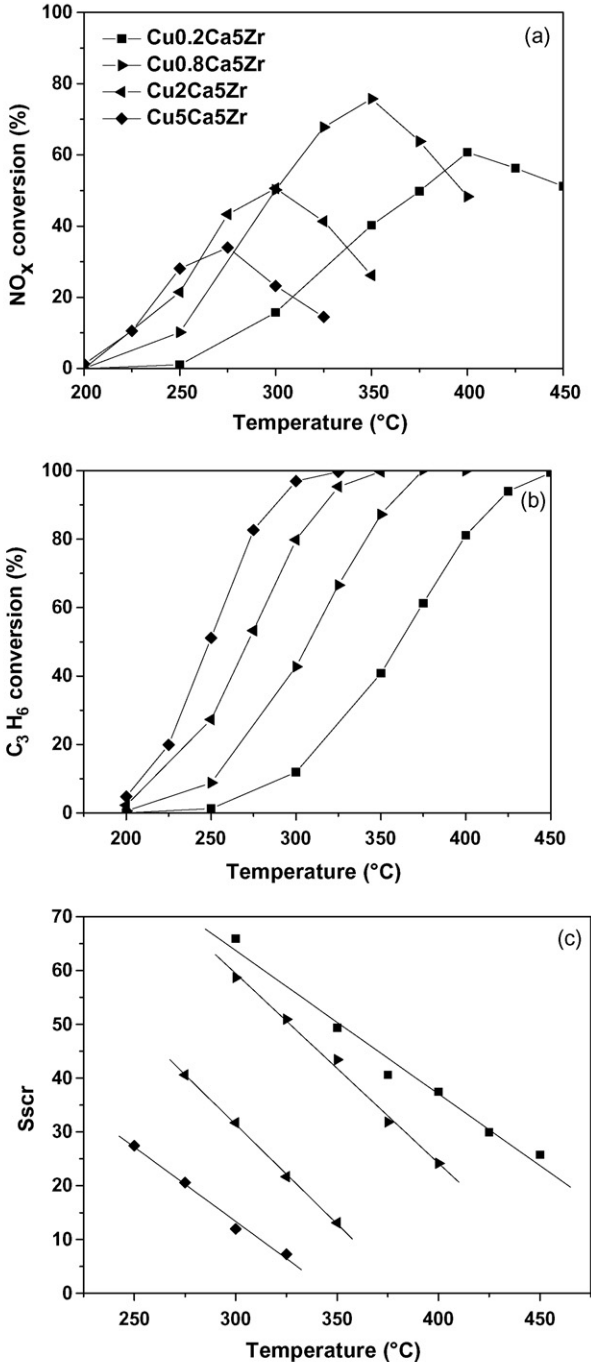

Fig. 3. (a) NO_x conversion, (b) C_3H_6 conversion, and (c) the selectivity S_{scr} profiles of CuCaZr catalysts with different copper loadings. The contents of Ca in the supports were 5 at.%. Catalyst weight 0.2 g, feed: 2000 ppm NO, 2000 ppm C_3H_6, 2% O_2, He balance and 120 mL min^{-1} total flow.

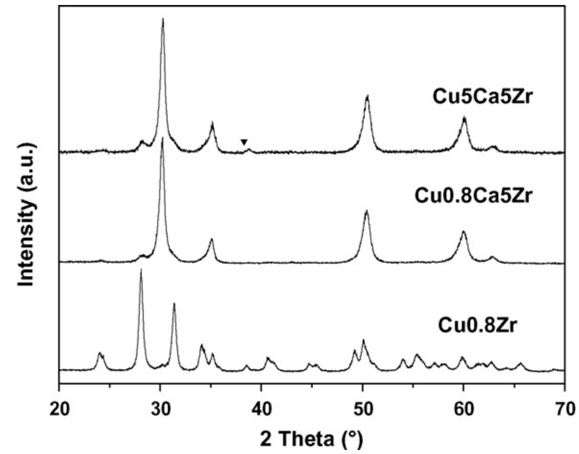

Fig. 4. XRD spectra of Cu0.8Zr, Cu0.8Ca5Zr, and Cu5Ca5Zr. (▼) CuO peak.

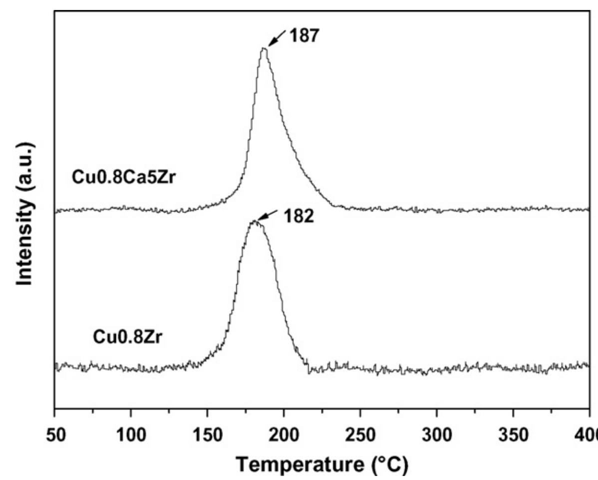

Fig. 5. H_2-TPR curves of Cu0.8Zr and Cu0.8Ca5Zr.

supported catalysts, tetragonal ZrO_2 was the main phase; the intensity of monoclinic ZrO_2 was weak but discernable, as shown on Cu0.8Ca5Zr and Cu5CaZr in Fig. 4. The BET surface area improvement of the modified CuZr catalysts noted above can be attributed to the crystal-phase change. Since tetragonal ZrO_2 is more stable than monoclinic ZrO_2 in maintaining the pore structure at high temperature. The small peak assigned to CuO was only identified over the Cu5Ca5Zr catalyst among all of catalysts in this study. The peak ascribed to alkaline-earth metal oxides was not observed in all the alkaline-earth metal modified samples.

3.2.3. *TPR*

The H_2-TPR profiles for Cu0.8Zr and Cu0.8Ca5Zr are shown in Fig. 5. Both of the two catalysts showed a unique reduction peak

Table 1
BET surface area, pore structure characterization of CuZr and modified CuZr catalysts

Samples	BET surface area ($m^2\ g^{-1}$)	Pore volume ($cm^3\ g^{-1}$)	Average pore diameter (nm)
CuZr	30	0.11	6.3
CuMgZr	42	0.14	4.0
CuSrZr	59	0.11	1.7
CuBaZr	47	0.09	1.8
CuCaZr	61	0.16	3.3

The loading of Cu over all of these catalysts was 0.8 wt%, and the contents of alkaline-earth metals in the supports were 5 at.%.

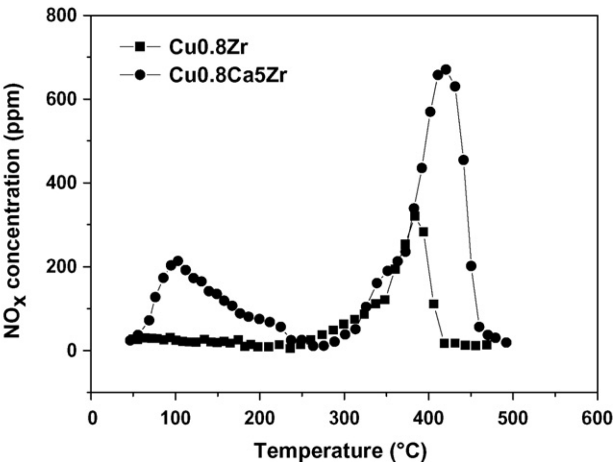

Fig. 6. NO_x-TPD profiles of Cu0.8Zr and Cu0.8Ca5Zr.

centered around 180 °C. The H_2-TPR peak of CuO crystalline phases always appears at temperatures above 250 °C [7,20]. According to observation of copper-based catalysts in other reports [12,21,22], the unique peak exhibited in this study was assigned to the presence of highly dispersed Cu^{2+} species in a single reduction step: $Cu^{2+} \rightarrow Cu^0$. It was noticed that the reduction temperature of the exposed Cu species for Cu0.8Ca5Zr catalyst shift to a higher temperature than that of Cu0.8Zr catalyst. XRD results have demonstrated the crystal phase change from monoclinic phase to tetragonal phase because of the addition of Ca to the support of the CuZr catalyst. This change might strengthen the metal–support interaction and produce new Cu species which are more resistant to reduction. The increased metal–support interaction could reduce the oxidation capacity of Cu species, which inhibited the side reaction of C_3H_6 oxidation in C_3H_6-SCR and promoted the activity of NO_x reduction.

3.2.4. NO_x-TPD

Fig. 6 illustrates the TPD profiles of NO_x on the Cu0.8Zr and Cu0.8Ca5Zr catalysts after adsorption mixture of 2000 ppm NO + 2% O_2. Cu0.8Zr catalyst showed single NO_x desorption peak centered at 380 °C which can be assigned to the decomposition of nitrate species. For Cu0.8Ca5Zr catalyst, two distinct desorption peaks of NO_x appeared located at 103 and 420 °C, respectively. The low temperature peak was always due to the decomposition of weakly bound nitrite species, but the high temperature peak was ascribed to the strongly bound nitrate species [23,24]. Since ad-NO_x species formed on the catalyst surface is known as an important role in NO reduction, NO_x ad-species desorbed above 350 °C are presumed to participate in NO reduction [25–27]. The amounts of NO_x desorption calculated from the desorption peak in the high temperature region are 57.6 and 140.7 μmol g^{-1} for Cu0.8Zr and Cu0.8Ca5Zr catalysts, respectively. Addition of alkaline-earth metal Ca to ZrO_2 support may improve both the strength and the number of basic sites over ZrO_2. As a consequence, acidic NO_x gas can be more easily adsorbed over CaZr than ZrO_2. This

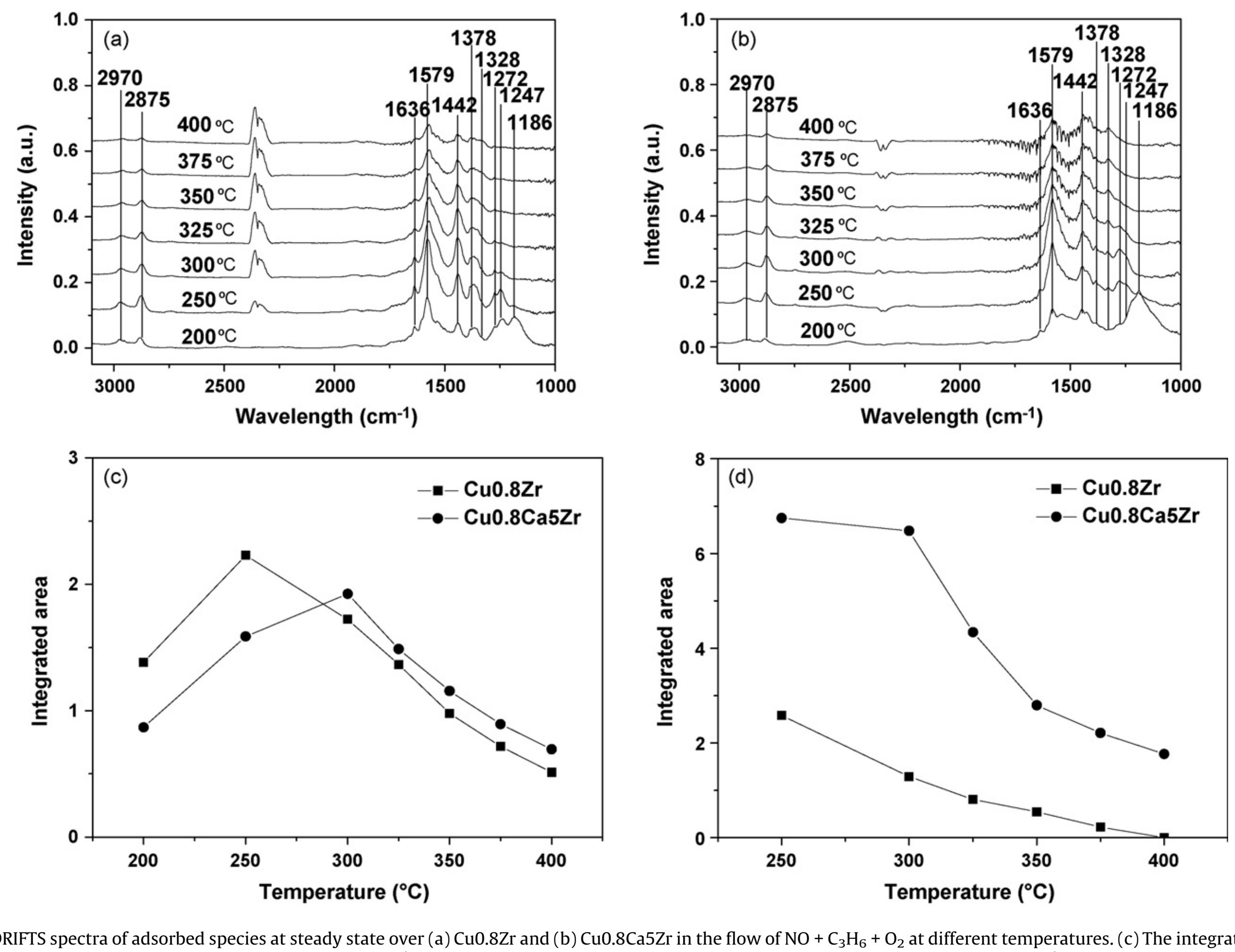

Fig. 7. DRIFTS spectra of adsorbed species at steady state over (a) Cu0.8Zr and (b) Cu0.8Ca5Zr in the flow of NO + C_3H_6 + O_2 at different temperatures. (c) The integrated areas of IR peaks for acetate species between 2800 and 2920 cm^{-1}. (d) The integrated areas of IR peaks for nitrate species between 1100 and 1307 cm^{-1}. Feed: 2000 ppm NO, 2000 ppm C_3H_6, 2% O_2, He balance and 120 mL min^{-1} total flow.

result can elucidate the promotion effect of Ca on the activity of CuZr catalyst in terms of the adsorption point of view.

3.2.5. DRIFTS

The difference of Cu0.8Zr and Cu0.8Ca5Zr catalysts for the SCR of NO_x was further investigated using DRIFTS. Fig. 7 shows the in situ DRIFTS spectra of these catalysts during the reaction of NO 2000 ppm + C_3H_6 2000 ppm + O_2 2% in a temperature range of 200–400 °C at the steady state.

After exposure of Cu0.8Zr catalyst to NO + C_3H_6 + O_2 reaction at various temperatures during the steady state, many bands appeared at 1186, 1247, 1272, 1328, 1378, 1442, 1579, 1636, 2875, and 2970 cm^{-1}. These bands were attributed to different intermediate species: nitrite (NO_2^-, 1186 cm^{-1}), monodentate nitrate (1247 cm^{-1}), bidentate nitrate (1272 cm^{-1}), acetate species (1378, 1442, 2875, and 2970 cm^{-1}), enolic species (1636 cm^{-1}) and carbonate species (1328 cm^{-1}) [28–31]. The peak at 1579 cm^{-1} was attributed to both acetate species (1580 cm^{-1}), and nitrate species (monodentate nitrate, 1539 cm^{-1}; bidentate nitrate, 1574 cm^{-1}). Nitrite species were only detected at 200 °C in the NO + C_3H_6 + O_2 reaction over Cu0.8Zr catalyst because they were unstable at high temperature. Monodentate nitrate and bidentate nitrate were the main ad-NO_x intermediate species for the reaction, and they coexisted at all of the testing temperatures. Acetate species were the main partially oxidized hydrocarbon intermediate species among all the detected oxidation hydrocarbon species. In particular, it was noted that NCO, CN, and RNO_2 species, which were always considered to be the key intermediate species in other catalytic systems, were not observed in this study. These species may be unstable on copper-based catalysts due to the high oxidation of copper species.

The DRIFTS spectrums of NO + C_3H_6 + O_2 reaction over Cu0.8Ca5Zr catalyst were shown in Fig. 7b. In similarity to the Cu0.8Zr catalyst, nitrite, monodentate nitrate, bidentate nitrate, acetate species, enolic species, and carbonate species were also detected in Cu0.8Ca5Zr catalyst at same wavelength positions.

The integrated areas of IR peaks for acetate species were shown in Fig. 7c. With the increase of temperature, the integrated area for acetate species over both Cu0.8Zr and Cu0.8Ca5Zr catalysts showed a peak value. At low temperature, activation of C_3H_6 to acetate species was difficult over the catalyst, while at high temperature, acetate species were oxidized to CO_2 and H_2O. Therefore, a peak content of adsorbed acetate species was obtained at a moderate temperature. Moreover, Cu0.8Ca5Zr catalyst showed smaller integrated area than Cu0.8Zr catalyst at temperature below 250 °C, but larger integrated area at high temperature zone indicated that addition of Ca to Cu0.8Zr catalyst reduced both the activation capacity and the oxidation capacity. This observation was consistent with the TPR results.

The integrated areas of IR peaks for nitrate species were shown in Fig. 7d. Both Cu0.8Zr and Cu0.8Ca5Zr catalysts showed a gradual decrease in the content of adsorbed nitrate species. However, the content of nitrate species over Cu0.8Ca5Zr was evidently much higher than that over Cu0.8Zr catalyst. This observation consistent with the NO_x-TPD measurement showed that Ca0.8Zr support could provide more nitrate than ZrO_2 even in the real reaction condition.

4. Conclusions

High promotional effect of alkaline-earth elements additive, especially Ca, on the catalytic performance of Cu/ZrO_2 catalyst were found in HC-SCR of NO_x reaction. Under the condition of 2000 ppm NO, 2000 ppm C_3H_6, and 2% O_2, the highest activity of 76% NO_x conversion was obtained over Cu0.8Ca5Zr catalyst at 350 °C. It was demonstrated that addition of Ca to the CuZr catalyst was beneficial to the copper dispersion and increased the metal–support interaction. This feature inhibited the side reaction of C_3H_6 oxidation and enhanced the C_3H_6 selectivity toward NO_x reduction. Moreover, the increase of the basic property on ZrO_2 support resulted from the addition of Ca could provide more ad-NO_x species for the SCR reaction. These explanations are all responsible for the promoting effect of Ca for the C_3H_6-SCR over CuZr catalyst.

Acknowledgements

This work was financially supported by the National Natural Science foundation of China (Grant NO. 20677034 and 20437010), and the National High-Tech Research and Development (863) Program of China (Grant No. 2006AA060301).

References

[1] C. TorreAbreu, M.F. Ribeiro, C. Henriques, F.R. Ribeiro, Appl. Catal. B 11 (1997) 383.
[2] C. Henriques, M.F. Ribeiro, C. Abreu, D.M. Murphy, F. Poignant, J. Saussey, J.C. Lavalley, Appl. Catal. B 16 (1998) 79.
[3] M. Shelef, C.N. Montreuil, H.W. Jen, Catal. Lett. 26 (1994) 277.
[4] K. Shimizu, H. Maeshima, A. Satsuma, T. Hattori, Appl. Catal. B 18 (1998) 163.
[5] M. Ozawa, H. Toda, O. Kato, S. Suzuki, Appl. Catal. B 8 (1996) 123.
[6] Y. Chi, S.S.C. Chuang, Catal. Today 62 (2000) 303.
[7] L.Y. Chen, T. Horiuchi, T. Osaki, T. Mori, Appl. Catal. B 23 (1999) 259.
[8] K.A. Bethke, M.C. Kung, B. Yang, M. Shah, D. Alt, C. Li, H.H. Kung, Catal. Today 26 (1995) 169.
[9] D. Pietrogiacomi, D. Sannino, S. Tuti, P. Ciambelli, V. Indovina, M. Occhiuzzi, F. Pepe, Appl. Catal. B 21 (1999) 141.
[10] A. Caballero, J.J. Morales, A.M. Cordon, J.P. Holgado, J.P. Espinos, A.R. Gonzalez-Elipe, J. Catal. 235 (2005) 295.
[11] H.H. Kung, M.C. Kung, Catal. Today 30 (1996) 5.
[12] P. Carniti, A. Gervasini, V.H. Modica, N. Ravasio, Appl. Catal. B 28 (2000) 175.
[13] G. Centi, S. Perathoner, D. Biglino, E. Giamello, J. Catal. 152 (1995) 75.
[14] S. Bennici, A. Gervasini, N. Ravasio, F. Zaccheria, J. Phys. Chem. B 107 (2003) 5168.
[15] N.A.S. Amin, E.F. Tan, Z.A. Manan, J. Catal. 222 (2004) 100.
[16] N.A.S. Amin, E.F. Tan, Z.A. Manan, Appl. Catal. B 43 (2003) 57.
[17] A. Auroux, D. Sprinceana, A. Gervasini, J. Catal. 195 (2000) 140.
[18] S. Bennici, P. Carniti, A. Gervasini, Catal. Lett. 98 (2004) 187.
[19] V. Indovina, D. Pietrogiacomi, M.C. Campa, Appl. Catal. B 39 (2002) 115.
[20] D. Terribile, A. Trovarelli, C. de Leitenburg, A. Primavera, G. Dolcetti, Catal. Today 47 (1999) 133.
[21] F. Boccuzzi, A. Chiorino, G. Martra, M. Gargano, N. Ravasio, B. Carrozzini, J. Catal. 165 (1997) 129.
[22] R.X. Zhou, T.M. Yu, X.Y. Jiang, F. Chen, X.M. Zheng, Appl. Surf. Sci. 148 (1999) 263.
[23] J.H. Li, J.M. Hao, X.Y. Cui, L.X. Fu, Catal. Lett. 103 (2005) 75.
[24] J.H. Li, J.M. Hao, L.X. Fu, T.L. Zhu, Z.M. Liu, X.Y. Cui, Appl. Catal. A 265 (2004) 43.
[25] T. Tanaka, T. Okuhara, M. Misono, Appl. Catal. B 4 (1994) L1.
[26] K. Shimizu, H. Kawabata, A. Satsuma, T. Hattori, J. Phys. Chem. B 103 (1999) 5240.
[27] M. Haneda, Y. Kintaichi, H. Hamada, Appl. Catal. B 20 (1999) 289.
[28] F.C. Meunier, J.P. Breen, V. Zuzaniuk, M. Olsson, J.R.H. Ross, J. Catal. 187 (1999) 493.
[29] H. He, J. Wang, Q.C. Feng, Y.B. Yu, K. Yoshida, Appl. Catal. B 46 (2003) 365.
[30] Y.W. Chi, S.S.C. Chuang, J. Catal. 190 (2000) 75.
[31] K. Shimizu, J. Shibata, H. Yoshida, A. Satsuma, T. Hattori, Appl. Catal. B 30 (2001) 151.